

Received October 3, 2020, accepted October 31, 2020, date of publication November 3, 2020, date of current version November 13, 2020.

Digital Object Identifier 10.1109/ACCESS.2020.3035670

# A Novel Reliability Analysis Approach With Collaborative Active Learning Strategy-Based Augmented RBF Metamodel

YANXU WEI<sup>1</sup>, GUANGCHEN BAI<sup>1</sup>, AND LU-KAI SONG<sup>1,2</sup> 

<sup>1</sup>School of Energy and Power Engineering, Beihang University, Beijing 100191, China

<sup>2</sup>Research Institute of Aero-Engine, Beihang University, Beijing 100191, China

Corresponding author: Lu-Kai Song (songlukai29@163.com)

This work was supported in part by the National Natural Science Foundation of China under Grant 51975028 and Grant 51575024, and in part by the Academic Excellence Foundation of Beihang University (BUAA) for Ph.D. Students under Grant BY1604137.

**ABSTRACT** Metamodels in lieu of time-demanding performance functions can accelerate the reliability analysis effectively. In this paper, we propose an efficient collaborative active learning strategy-based augmented radial basis function metamodel (CAL-ARBF), for reliability analysis with implicit and nonlinear performance functions. For generating the suitable samples, a CAL function is first designed to constrain the new samples being generated in sensitivity region, near limit state surface and keep certain distances mutually. Then by adjusting the adjustment coefficient of CAL function, the CAL-ARBF is mathematically modeled and the corresponding reliability analysis theory is developed. The effectiveness of the proposed approach is validated by four numerical samples, including global nonlinear problem, local nonlinear problem, nonlinear oscillator and truss structure. Through comparison of several state-of-the-art methods, the proposed CAL-ARBF is demonstrated to possess the computational advantages in efficiency and accuracy for reliability analysis.

**INDEX TERMS** Active learning function, radial basis function, reliability analysis, metamodel.


## I. INTRODUCTION

Various uncertainties widely exist in real structural engineering such as aerospace equipment, mechanical component and civil structure [1]–[4]. Reliability analysis is an effective way to address these uncertainties and ensure structural safety [5]–[10]. In general, the reliability analysis is to calculate the failure probability using the limit state function (LSF) and probabilistic information of random variables. At present, considerable reliability analysis methods have been developed to estimate failure probability. The first-order and the second-order reliability methods (FORM and SORM) can acquire failure probability by approximating the LSF around the most probable point (MPP). However, the computational error of these reliability analysis methods tends to be unacceptable for highly nonlinear and/or implicit functions. Monte Carlo Simulation [11] (MCS) provides a powerful and robust alternative to evaluate the failure probability whether the performance functions are implicit or explicit. Nevertheless, owing to its statistical principles,

MCS requires enormous evaluations of performance functions and thereby leads to prohibitively expensive computational costs, especially for complex engineering with low failure probability.

Under the circumstances, to decrease the expensive computational cost, metamodels (or surrogate models) combined with MCS have been emerged and widely applied in reliability analysis [12]–[14]. The classic metamodels include artificial neural network (ANN) [15]–[17], support vector machine (SVM) [18], [19], Kriging model [20], [21], radial basis function [22], [23] (RBF) and exponential surrogate model [24]. Among them, as one of accurate interpolation methods, RBF can efficiently deal with high dimensional problems with exponentially converge rate [25]–[27] and the Gaussian function-based augmented RBF (ARBF) is one of the most widely used RBF, which can make full use of all the samples and possesses potentials to accomplish an accurate approximation [28]. So it had been widely applied in reliability evaluation and design fields [22], [25]–[28].

Apart from metamodel selection, the samples generation strategy is another critical part to ensure the accuracy and

The associate editor coordinating the review of this manuscript and approving it for publication was Jiajie Fan .

efficiency of metamodel for reliability analysis, because appropriate sample sets can acquire more accurate description about LSF. At present, samples generation strategies are usually classified into two types, i.e., one-shot sampling and adaptive sequential sampling [29], [30]. Compared with one-shot sampling generating all samples in advance, the adaptive sequential sampling generates one or more samples at each iteration with the guidance information provided by the existing samples and metamodel, which can assure excellent samples distribution and therefore improves the efficiency and accuracy of metamodel [31]–[44]. Active learning strategy provides excellent approach to complete the adaptive sequential sampling, which were widely applied many fields such as global sensitivity analysis [45], remote sensing [46], [47] and geostatistics [23], [48]. Most of them require accurate approximations overall a certain limited region. Different from these fields, reliability analysis requires an accurate approximation to the limit state function in the high probability density region [31]–[40], which requires that the active learning strategy should generate samples close to the limit state function in the high probability density region [49]. As the core of active learning strategy, active learning function plays the vital role in guiding samples generation in each iteration [49]–[51]. However, only through the existing active learning functions, it is hard to effectively constrain the samples close to LSF overall the sensitive region (the region around MPP as shown in Fig. 1) and keep certain distances mutually, which may lead to poor sample quality, inefficiency or inaccuracy for metamodeling.

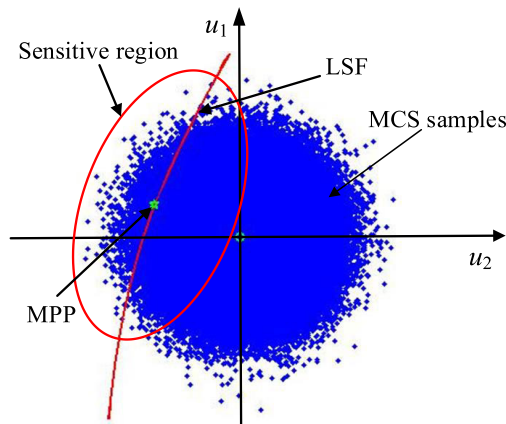


FIGURE 1. Sketch of sensitive region.

To overcome the defects, to the best of authors' knowledge, the main challenge is how to generate samples conforming to the following constraints: 1) region constraint: samples should be constrained in sensitive region to avoid wasted calls of performance function; 2) surface constraint: samples should be close to LSF to improve the local description of performance function; 3) distance constraint: samples should be kept certain distances to enhance numerical stabilities and global fitting precision overall sensitive region. Obviously,

the generated samples concurrently conforming to the three constraints can acquire appropriate samples and accomplish high-accuracy and high-efficiency metamodeling. To meet these constraints and generate appropriate samples, it is urgently desired to develop a novel active learning function to achieve efficient and accurate reliability analysis.

In this study, to meet these constraints and generate appropriate samples, a collaborative active learning (CAL) strategy is proposed. In this CAL strategy, three control functions (i.e., region control function, surface control function and distance control function) are first developed to mathematically describe the three constraints respectively; subsequently, to organically balance the influence of the three constraints on generated samples, a unified framework is further designed through a collaborative optimal function (CAL function); finally, by adjusting the adjustment coefficient of CAL function, the appropriate samples (i.e., located in sensitive region, near limit state function and keep certain distances mutually) can be obtained by several stages. Moreover, by fusing CAL strategy and ARBF model, the CAL-ARBF metamodel is mathematically constructed. The effectiveness of the presented metamodel are validated by four numerical samples.

The rest of this paper is organized as follows: Section 2 investigates the basic theory of the presented approach including augmented RBF model, CAL strategy and metamodel-based reliability analysis. Section 3 validates the developed method by four numerical examples. Some conclusions are summarized in Section 4.

## II. CAL-ARBF METHOD

### A. AUGMENTED RBF MODEL, ARBF

Radial basis function (RBF) model is an exact interpolation algorithm, which can fit the highly nonlinear performance function with high fitting precision. As one important form of RBF model, ARBF model can improve the adaptability of RBF model in fitting complex performance functions. In view of these virtues, the ARBF model is employed to construct the metamodel in this paper. The basic principle of ARBF model is introduced as follows.

For a given sample set  $\mathbf{X} = (\mathbf{x}_1, \mathbf{x}_2, \dots, \mathbf{x}_i, \dots, \mathbf{x}_m)$ , the RBF model  $g_r(\mathbf{x})$  is constructed by linear combination of  $m$  radial basis functions:

$$g_r(\mathbf{x}) = \sum_{i=1}^m a_i \phi(\|\mathbf{x} - \mathbf{x}_i\|_2, c) \quad (1)$$

where  $a_i$  indicates the expansion coefficient of RBF model;  $\phi(\mathbf{x})$  the Gaussian RBF function in this paper;  $\|\mathbf{x} - \mathbf{x}_i\|_2$  the Euclidean distance from  $\mathbf{x}$  to  $\mathbf{x}_i$ ;  $c$  the shape parameter, which holds a great influence on RBF accuracy. In this study, the cross-validation technique is employed to obtain the value of shape parameter  $c$  [22].

To improve the fitting ability of RBF model for complex performance functions, an augmented function term  $g_p(\mathbf{x})$  is introduced into the above RBF model. The new ARBF model

$g_{ar}(\mathbf{x})$  is expressed as:

$$g_{ar}(\mathbf{x}) = \sum_{i=1}^m a_i \phi(\|\mathbf{x} - \mathbf{x}_i\|_2, c) + \sum_{j=1}^p b_j g_{pj}(\mathbf{x}) \quad (2)$$

where  $b_j$  indicates the  $j$ -th coefficient of  $g_p(\mathbf{x})$ .  $p$  the number of augmented terms. Moreover, to address the underdetermined equation problems brought by augmented terms, an additional orthogonality condition is introduced:

$$\sum_{i=1}^m a_i g_{pj}(\mathbf{x}_i) = 0 \quad j = 1, 2, \dots, p \quad (3)$$

Then the corresponding undetermined coefficients of ARBF model can be obtained by solving the following simultaneous equations:

$$\begin{pmatrix} \mathbf{A} & \mathbf{G} \\ \mathbf{G}^T & \mathbf{0} \end{pmatrix} \begin{pmatrix} \mathbf{a} \\ \mathbf{b} \end{pmatrix} = \begin{pmatrix} \mathbf{g} \\ \mathbf{0} \end{pmatrix} \quad (4)$$

where  $\mathbf{G}$  is the matrix format of the augmented function term  $G_{i,j} = g_{pj}(\mathbf{x}_i)$  ( $i = 1, 2, \dots, m; j = 1, 2, \dots, p$ );  $\mathbf{A}$  the matrix form of RBFs  $A_{i,j} = A_{j,i} = \phi(\|\mathbf{x}_j - \mathbf{x}_i\|_2, c)$  ( $i = 1, 2, \dots, m; j = 1, 2, \dots, p$ );  $\mathbf{a}$  and  $\mathbf{b}$  the matrix format of  $a_i$  and  $b_j$ .  $\mathbf{g}$  the vector of the performance function values.

Noticeably, for structural reliability analysis with implicit and nonlinear traits, the augmented RBF model possesses the potentials to approximate the complex LSF accurately, so long as the suitable and efficient sample set is provided.

### B. COLLABORATIVE ACTIVE LEARNING STRATEGY, CAL

Since the sample set has a key influence on the accuracy and efficiency of metamodel, in this subsection, a collaborative active learning (CAL) strategy is proposed to generate appropriate samples, which includes initial samples selection, CAL function design and new samples generation.

#### 1) INITIAL SAMPLES SELECTION

To provide some elementary information of performance function, a small group of initial samples ( $n + 1$  samples, where  $n$  means the variables dimension) are first generated by deterministic selection technique [12]. Herein, the  $i$ -th generated sample  $\mathbf{x}_i$  is expressed as:

$$\mathbf{x}_i = [x_{m1}, x_{m2}, \dots, x_{mi} - f\sigma_i, \dots, x_{mn}] \quad i = 1, 2, \dots, n \quad (5)$$

where  $x_{mi}$  means the mean value of the  $i$ -th input variable;  $\sigma_i$  the standard deviation of the  $i$ -th input variable;  $f$  the selecting coefficient whose value is chosen as 1.5, to seek for informative samples around the mean values along the axis  $x_i$  [6], [12]–[14]. Together with  $\mathbf{x}_m$ ,  $n + 1$  samples are selected.

To improve the space distribution performance of initial samples, by using the above  $n + 1$  samples and their performance function values  $\mathbf{g}$ , a new center point (NCP) with good distribution performance is generated [6]. Together with the above  $n + 1$  samples,  $n + 2$  samples are generated

and treated as the initial samples. Through the deterministic selection technique, the stochastic fluctuations are eliminated effectively and the initial samples are generated reasonably. Moreover, the excellent space distribution performance of initial samples can also provide a promising way to generate appropriate new samples.

#### 2) CAL FUNCTION DESIGN

To guide new appropriate sample generation, a CAL function is proposed. The CAL function based new sample generation sketch is drawn in Fig. 2. The basic thought of CAL function is: in sample generation process, the sample constraints are first decomposed into three sub constraints (i.e., region constraint, surface constraint and distance constraint) and mathematically described by three corresponding control functions (i.e., region control function, surface control function and distance control function). Afterwards, to organically balance the effect of the three constraints on samples, a collaborative optimal function (CAL function) is formulated by collaborating the three control functions into one unified framework with an adjustment coefficient  $\lambda$ . Subsequently, along with minimizing the values of CAL function, the new appropriate sample  $\mathbf{x}_s$  are generated. The design process of CAL function (i.e., region control function, surface control function and distance control function, collaborative optimal function) is presented as follows.

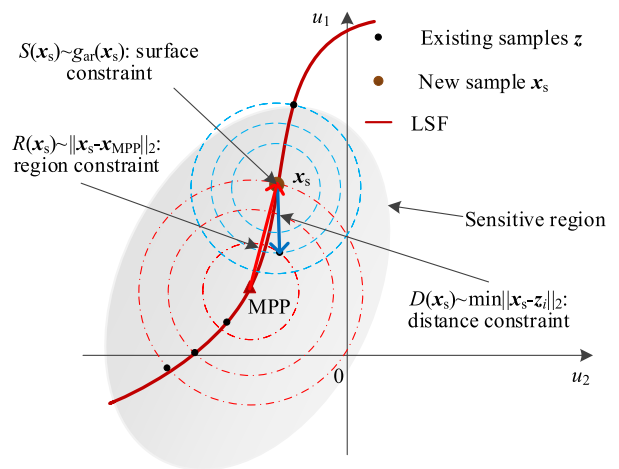


FIGURE 2. Sketch of CAL function in two dimensional coordinates.

#### a: REGION CONTROL FUNCTION

As shown in Fig.1 and Fig.2, since the sensitive region contains the LSF in the high probability density region, samples is required to be generated in this region to avoid the useless calls of performance functions. To constrain new samples in sensitive region, the Euclidean distance  $\|\mathbf{x}_s - \mathbf{x}_{MPP}\|_2$  (the red solid line shown in Fig. 2) from the new sample  $\mathbf{x}_s$  to the evaluated  $\mathbf{x}_{MPP}$  is employed. Moreover, to keep the data unity in various problems, the Euclidean distance is transformed into standard normal space. Then the region control function

$R(\mathbf{x}_s)$  is designed as:

$$R(\mathbf{x}_s) = \sqrt{\sum_{l=1}^n \left[ \frac{(x_{sl} - x_{ml})}{\sigma_l} - \frac{(x_{MPPl} - x_{ml})}{\sigma_l} \right]^2} \quad (6)$$

where  $x_{sl}$  indicates the  $l$ -th component of the new sample  $\mathbf{x}_s$ ;  $x_{MPPl}$  the  $l$ -th component of the MPP  $\mathbf{x}_{MPP}$ ;  $x_{ml}$  the  $l$ -th component of the mean value  $\mathbf{x}_m$ ;  $\sigma_l$  the standard deviation of the  $l$ -th input variable. Through adjusting the value of the region control function  $R(\mathbf{x}_s)$ , the new samples shall be efficiently settled down in sensitive region.

*b: SURFACE CONTROL FUNCTION*

The MCS samples close to LSF are great challenges for the accuracy of failure probability evaluated by metamodel since the sign of them are difficult to evaluate precisely. Moreover, samples close to LSF contribute the most to the fitting precision of metamodel. Therefore, samples are demanded to be generated near LSF. By following this request, since the existed metamodel  $g_{ar}(\mathbf{x})$  obtained with the existing samples can approximate LSF accurately to a certain extent, the  $g_{ar}(\mathbf{x}_s)$  at the new sample  $\mathbf{x}_s$  is employed to develop the surface control function  $S(\mathbf{x}_s)$ , which is expressed as:

$$S(\mathbf{x}_s) = \sum_{i=1}^m a_i \phi(\|\mathbf{x}_s - \mathbf{z}_i\|_2, c) + \sum_{j=1}^p b_j g_{pj}(\mathbf{x}_s) \quad (7)$$

$m$  is the number of existing samples. Through minimizing the absolute value of surface control function  $|S(\mathbf{x}_s)|$ , the new samples will be effectively kept close to LSF. It should be noted that with the increase of samples iteratively, the metamodel will achieve higher fitting precision to LSF and thereby gradually improve the quality of surface control function  $S(\mathbf{x}_s)$ .

*c: DISTANCE CONTROL FUNCTION*

For evaluating the metamodel, samples overlapping or being particularly close to each other would lead to numerical instabilities and wasted simulations. In addition, to accurately and efficiently accomplish metamodel overall the sensitive region, the generated samples should keep a certain distance and fill in the sensitive region as well. Accordingly, to keep the samples distant with each other, the minimum Euclidean distance  $\|\mathbf{x}_s - \mathbf{z}_i\|_2$  (the blue solid line shown in Fig. 2) from the new sample  $\mathbf{x}_s$  to the existing samples  $\mathbf{z}_i$  is used to develop a distance control function  $D(\mathbf{x}_s)$ . Similar to region control function definition, the  $D(\mathbf{x}_s)$  is formulated in standard normal space:

$$D(\mathbf{x}_s) = \min_{z_i} \sqrt{\sum_{l=1}^n \left[ \frac{(x_{sl} - x_{ml})}{\sigma_l} - \frac{(z_{il} - x_{ml})}{\sigma_l} \right]^2} \quad (8)$$

where  $z_{il}$  is the  $l$ -th component of the  $i$ -th existing samples and  $i = 1, 2, 3, \dots, m$ . Clearly, with maximizing the value of distance control function  $D(\mathbf{x}_s)$ , the generated samples can be located distant with each other.

*d: COLLABORATIVE OPTIMAL FUNCTION*

Through the three independent control functions defined above, the related region, surface and distance constraints can be achieved respectively. However, each control function can achieve a part of the samples constraints and cannot determine the new samples alone. Therefore, the three control functions must be collaborated and compromised with each other through a unified framework, to generate the new samples.

On this condition, collaborating the optimization goals of the three control functions by their pretreatments, a collaborative optimal function  $C(\mathbf{x}_s)$  is defined. To improve the flexibility of  $C(\mathbf{x}_s)$ , an adjustment coefficient  $\lambda$  is introduced. The  $C(\mathbf{x}_s)$  is expressed as:

$$C(\mathbf{x}_s) = \min_{\mathbf{x}_s} \left[ \lambda R(\mathbf{x}_s) + (1 - \lambda) |S(\mathbf{x}_s)| + \frac{1}{D(\mathbf{x}_s)} \right] \quad (9)$$

Equation (9) is the CAL function. The adjustment coefficient  $\lambda$  is defined as  $\lambda \in (0, 1)$  to decrease the region constraint to keep the distance between new sample to existing samples  $\mathbf{z}$ . The coefficient  $1 - \lambda$  can decrease the surface control function and thereby further enhance the role of  $\lambda$  in Eq. (9). It should be noted that the optimal solution of the CAL function is not the optimal solution of any control functions as possible as it can, i.e., it can meet the three control functions to a certain extent simultaneously.

At each iteration, the new sample  $\mathbf{x}_s$  can be acquired through optimizing the CAL function based on the MCS samples or with non-gradient optimal algorithm such as genetic algorithm, particle swarm optimization algorithm, artificial bee colony algorithm, etc. [52]–[58].

3) NEW SAMPLES GENERATION

As shown in (9), within the defined interval, a large value of adjustment coefficient  $\lambda$  can enhance the region constraint and thereby keep the new samples located close to MPP, whereas a small one can lead to the opposite results. Therefore, through adjusting the value of adjustment coefficient  $\lambda$ , the samples generation trends are controlled and new appropriate samples are generated to accomplish the approximation iteratively. The samples generation process is summarized in three stages:

*a: NCP APPROXIMATION*

Since the new center point (NCP) can meet the samples constraints roughly, new samples generated around NCP are more compliant with samples constraints, so new samples are generated around NCP first by enhancing the region constraint and regarding the NCP as MPP, to accomplish the NCP approximation. Therefore, the adjustment coefficient  $\lambda$  is defined as  $\lambda^* \in (0.5, 1)$ .

*b: GLOBAL APPROXIMATION*

To enhance the overall distribution performance of new generated samples, the adjustment coefficient  $\lambda$  in this stage is

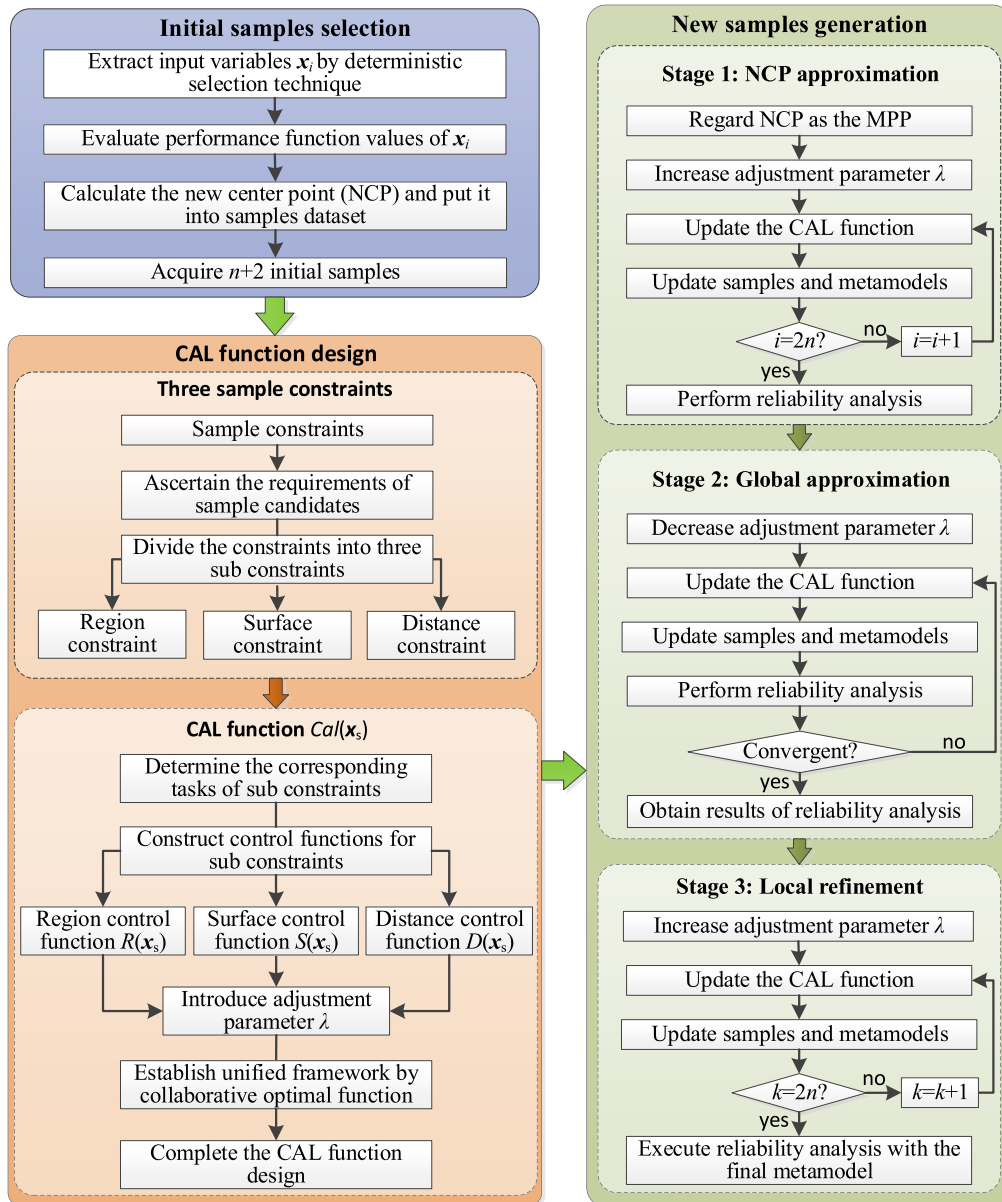


FIGURE 3. Flowchart of CAL-ARBF metamodeling.

set as  $(1-\lambda^*) \in (0, 0.5)$  to decrease the region constraint and thereby new samples can be generated dispersedly around MPP to complete the global approximation overall sensitive region.

### c: LOCAL REFINEMENT

Due to the decrease of the region constraint in stage 2, the possibility of an inaccurate approximation around MPP still exists, so local refinement around MPP is introduced by increasing adjustment coefficient  $\lambda$  as  $\lambda^* \in (0.5, 1)$ .

The flowchart of CAL-ARBF metamodeling is shown in Fig. 3 in detail.

### C. METAMODEL-BASED RELIABILITY ANALYSIS THEORY

In this section, by integrating virtues of ARBF model and CAL strategy, the CAL-ARBF metamodeling, the corresponding reliability analysis theory, and the benefits of the proposed approach are presented.

#### 1) CAL-ARBF METAMODELING

Assuming that  $z_{ini}$  is the initial samples and  $g_{ini}$  is the corresponding values of performance function, the samples in  $k$ -th iteration can be expressed as  $z^k = (z_{ini}, x_1, x_2, \dots, x_k)$  and their performance function values are  $g_{exi}^k = (g_{ini}, g_1, g_2, g_3, \dots, g_k)$ . Herein, the CAL-ARBF metamodel  $g_{ar}^k$



in  $k$ -th iteration is established as:

$$g_{ar}^k(\mathbf{x}) = \sum_{i=1}^m a_i^k \phi(\|\mathbf{x} - \mathbf{z}_i\|_2, c^k) + \sum_{j=1}^{n+1} b_j^k g_{pj}(\mathbf{x}) \quad (10)$$

Then the  $(k + 1)$ -th surface control function  $S^{k+1}(\mathbf{x}_s^{k+1})$  is established as:

$$S^{k+1}(\mathbf{x}_s^{k+1}) = \sum_{i=1}^m a_i^k \phi(\|\mathbf{x}_s^{k+1} - \mathbf{z}_i\|_2, c^k) + \sum_{j=1}^{n+1} b_j^k g_{pj}(\mathbf{x}_s^{k+1}) \quad (11)$$

Similarly, according to the Euclidean distance  $\|\mathbf{x}_s^{k+1} - \mathbf{x}_{MPP}^k\|_2$  and the minimum Euclidean distance  $\min\|\mathbf{x}_s^{k+1} - \mathbf{z}_i^k\|_2$ , the  $(k + 1)$ -th region control function  $R^{k+1}(\mathbf{x}_s^{k+1})$  and the  $(k + 1)$ -th surface control function  $D^{k+1}(\mathbf{x}_s^{k+1})$  are constructed as:

$$R^{k+1}(\mathbf{x}_s^{k+1}) = \sqrt{\sum_{l=1}^n \left[ \frac{(x_{sl}^{k+1} - x_{ml})}{\sigma_k} - \frac{(x_{MPPl}^k - x_{ml})}{\sigma_k} \right]^2} \quad (12)$$

$$D^{k+1}(\mathbf{x}_s^{k+1}) = \min_{z^i} \sqrt{\sum_{l=1}^n \left[ \frac{(x_{sl}^{k+1} - x_{ml})}{\sigma_k} - \frac{(z_{il} - x_{ml})}{\sigma_k} \right]^2} \quad (13)$$

Collaborating the  $S^{k+1}(\mathbf{x}_s^{k+1})$ ,  $R^{k+1}(\mathbf{x}_s^{k+1})$ , and  $D^{k+1}(\mathbf{x}_s^{k+1})$  with (9), the  $(k + 1)$ -th CAL function  $C^{k+1}(\mathbf{x}_s^{k+1})$  is:

$$C^{k+1}(\mathbf{x}_s^{k+1}) = \min_{\mathbf{x}_s^{k+1}} \left[ \lambda R^{k+1}(\mathbf{x}_s^{k+1}) + (1 - \lambda) \left| S^{k+1}(\mathbf{x}_s^{k+1}) \right| + \frac{1}{D^{k+1}(\mathbf{x}_s^{k+1})} \right] \quad (14)$$

By solving the optimization problem (14), the new sample  $\mathbf{x}_s^{k+1}$  is generated and the  $k$ -th sample set  $\mathbf{z}^k$  is updated as  $\mathbf{z}^{k+1} = (\mathbf{z}_{ini}, \mathbf{x}_1, \mathbf{x}_2, \dots, \mathbf{x}_k, \mathbf{x}_{k+1})$ . Then the  $(k + 1)$ -th CAL-ARBF metamodel  $g_{ar}^{k+1}(\mathbf{x})$  can be constructed correspondingly.

With enough iterative calculations, an accurate CAL-ARBF metamodel can be constructed finally.

## 2) RELIABILITY ANALYSIS THEORY

In this subsection, based on the constructed CAL-ARBF metamodel and Monte Carlo simulation, the structural reliability analysis is executed. To evaluate the failure probability, a large group of MCS samples are first generated. Then according to the  $k$ -th CAL-ARBF metamodel  $g_{ar}^k(\mathbf{x})$  and the MCS samples, the failure probability in the  $k$ -th iteration is evaluated as:

$$p_f^k = \frac{1}{n_{MCS}} \sum_{i=1}^{n_{MCS}} I[g_{ar}^k(\mathbf{x}^i) < 0] \quad (15)$$

where  $n_{MCS}$  denotes the number of MCS samples;  $I[\cdot]$  the indicator function, which is equal to 1 when  $g_{ar}^k(\mathbf{x}) < 0$  and 0 when  $g_{ar}^k(\mathbf{x}) \geq 0$ .

To control the iterations while maintaining acceptable accuracy, the corresponding stopping criteria of structural reliability analysis is defined as:

$$\left| \frac{p_f^k - p_f^{k-1}}{p_f^k} \right| < \varepsilon \quad (16)$$

where  $p_f^k$  and  $p_f^{k-1}$  the  $k$ -th and  $(k - 1)$ -th failure probability;  $\varepsilon$  the termination number, which is a small positive number. It set as  $10^{-4}$  to ensure the accuracy of four significant digits of the failure probability. In addition, due to that only one sample is added into the sample set in each iteration, the evaluation process may be terminated with a small sample set and thereby lead to an inaccurate result. To overcome this defect, a minimum number of samples ( $5n$  samples) is defined to ensure the simulation accuracy. Once the stopping criterion is satisfied, the final failure probability can be obtained in stage 2.

## 3) BASIC BENEFITS OF CAL-ARBF

From the analysis above, the proposed CAL-ARBF metamodel possesses potentials to accomplish reliability analysis accurately and efficiently, the basic benefits of which are summarized as follows.

1) ARBF model can adapt to the complexity of functions and effectively use samples' information, which provides the possibility of enhancing approximation accuracy.

2) Stochastic fluctuations of initial samples are eliminated by deterministic selection technique, which enhances the data stability of the proposed approach.

3) Samples constraints are divided into three sub constraints, which simplify the complexity degree of generating appropriate samples.

4) These sub constraints are mathematically described by three control functions, which can effectively achieve the corresponding sub samples constraint.

5) CAL function is designed by collaborating the three control functions with an adjustment coefficient, which can balance the influence of the three sub constraints on samples.

6) By fusing the virtues of CAL strategy and ARBF model, the presented CAL-ARBF metamodel holds the potentials to perform the reliability analysis accurately and efficiently.

## III. NUMERICAL EXAMPLES

In this section, four numerical reliability analysis examples are discussed to illustrate the efficiency and accuracy of the presented CAL-ARBF approach, including global nonlinear problem, local nonlinear problem, nonlinear oscillator and truss structure. Note that the theoretical performance function problems (i.e., global nonlinear problem and local nonlinear problem) are utilized to visualize the samples generation process and CAL-ARBF metamodeling process, and the practical performance function problems (i.e., nonlinear oscillator

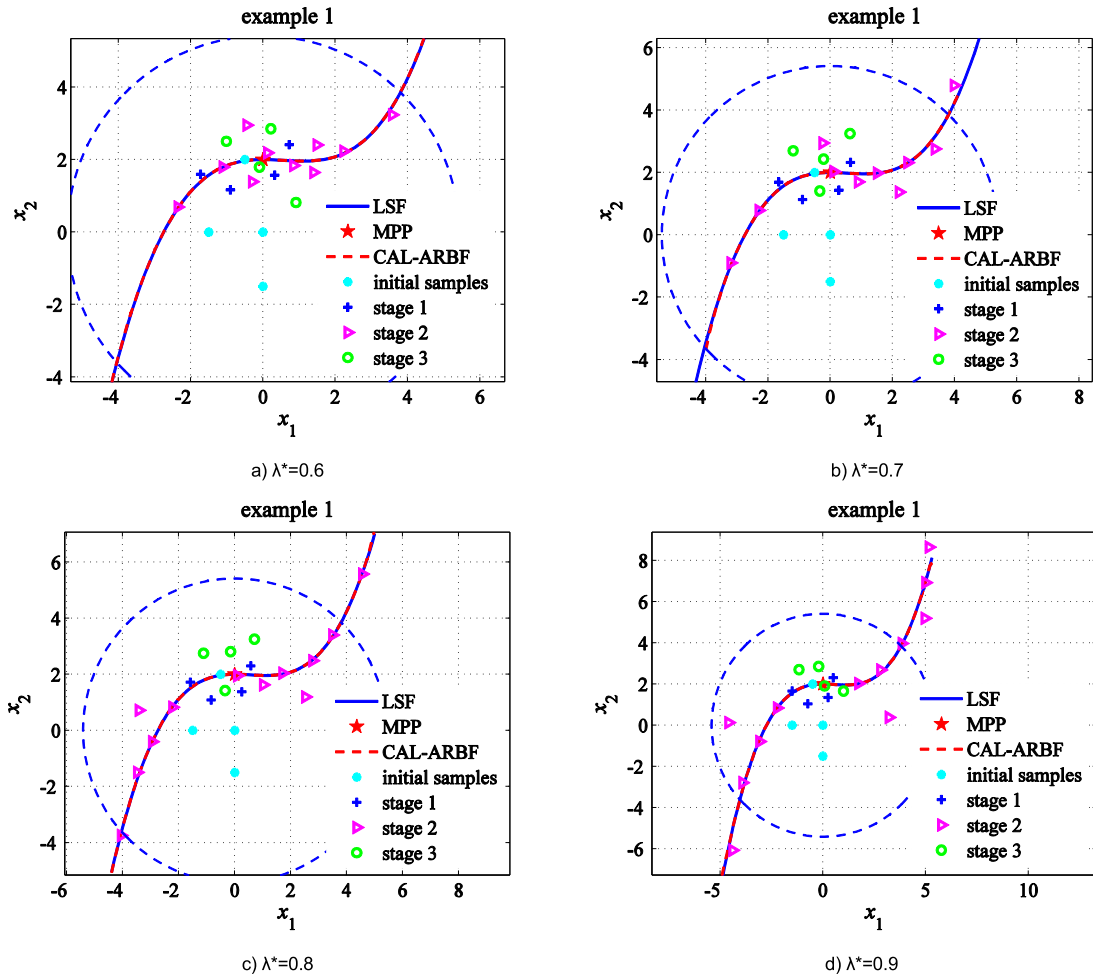


FIGURE 4. Sample distribution with different adjustment coefficients (example 1).

and truss structure) are employed to validate the engineering application of the developed CAL-ARBF approach. Moreover, to eliminate the influence of randomness on the validation of the proposed method, the initial samples are generated by deterministic generation method; the same MCS samples, which is sufficient to eliminate the randomness in sampling techniques, are generated to perform reliability analysis. The accuracy of failure probability is used as the accuracy of the proposed method, and the number of design samples is used to represent the efficiency of the proposed method.

**A. EXAMPLE 1: A GLOBAL NONLINEAR PROBLEM**

To demonstrate global nonlinear approximation ability of proposed method in sensitive region, a global nonlinear problem overall sensitive region [14], [24] is used:

$$g(\mathbf{x}) = 2 - x_2 - 0.1x_1^2 + 0.06x_1^3 \quad (17)$$

where  $x_1$  and  $x_2$  are two independent input variables with standard normal distribution.

To reveal the influence of the adjustment coefficient  $\lambda$  on samples distribution and reliability analysis results, the CAL-ARBF metamodeling is performed by using different

adjustment coefficients (i.e.,  $\lambda^* = 0.6, 0.7, 0.8, 0.9$ ). The samples distribution and reliability analysis results are obtained in Fig. 4 and Table 1 respectively. Note that the blue dotted line arcs in Fig. 4 represent the high probability density region, and the radius is determined by  $\max\|\mathbf{x}_{MCS_i}\|_2$ .

As shown in Fig. 4, a large adjustment coefficient  $\lambda$  is beneficial to generating samples gathering around NCP and MPP, whereas a small adjustment coefficient  $\lambda$  can keep samples distant with each other. Nevertheless, in stage 2 ( $\lambda = 1 - \lambda^*$ ), a too large value of adjustment coefficient (i.e., in Fig. 4 (a)) would lead to the new samples cannot fill the sensitive region and may influence the computational accuracy, whereas a too small value (i.e., in Fig. 4 (d)) will make some of the samples out of the sensitive region and decrease the computational efficiency. Therefore, the value of adjustment coefficient should be limited as the proposed method does, especially in stage 2. As shown in Table 1, despite the slight difference in simulation efficiency, the simulation accuracy is similarly high for this example, which shows the defined adjustment coefficient value holds robustness in performing reliability analysis.

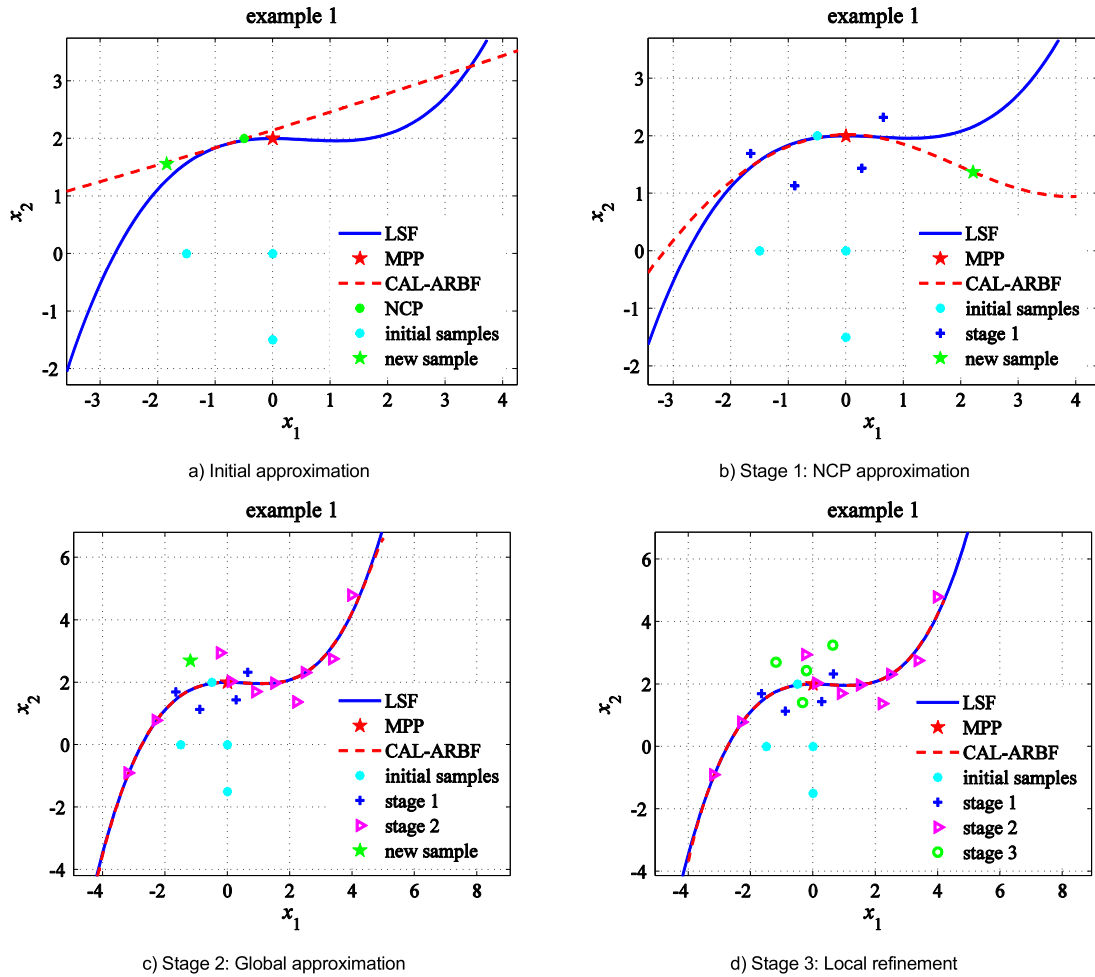


FIGURE 5. Metamodeling stages of CAL-ARBF (example 1,  $\lambda^* = 0.7$ ).

TABLE 1. Results of failure probabilities with different adjustment coefficients (example 1).

Method	$p_f (10^{-2})$	$N_s$	$C_v (10^{-2})$	$\delta_1 (10^{-4})$
Direct MCS	3.443	$5 \times 10^6$	0.237	—
CAL-ARBF ( $\lambda^*=0.6$ )	3.443	22	0.237	0
CAL-ARBF ( $\lambda^*=0.7$ )	3.443	22	0.237	0
CAL-ARBF ( $\lambda^*=0.8$ )	3.443	24	0.237	0
CAL-ARBF ( $\lambda^*=0.9$ )	3.443	24	0.237	0

The coefficient of variation  $C_v$  indicates the uncertainty on failure probability and  $C_v = \sqrt{(1 - p_f) / p_f n_{MCS}}$ ;  $N_s$  represents the number of samples;  $\delta_1$  is evaluated by  $|p_f - p_{ef}| / p_{ef}$ , where  $p_{ef}$  the failure probability obtained by direct MCS method.

To illustrate the CAL-ARBF metamodeling procedure, the CAL-ARBF with  $\lambda^* = 0.7$  is introduced in detail. The different metamodeling stages of CAL-ARBF are shown in Fig. 5. Herein, the detailed metamodeling process is summarized as:

For initialization as shown in Fig. 5 a), it is clear that the NCP is close to LSF and the metamodel is relatively accurate around NCP, so the four samples generated around NCP in stage 1 are more conforming to samples constraints

as shown in Fig. 5 b). Then the fitting precision is improved iteratively, which provides more useful information for generating samples overall the sensitive region. Therefore, in stage 2, scattered samples are generated with decreasing the region constraint and thereby the metamodel can approximate the LSF accurately overall the sensitive region as shown in Fig. 5 c). At last in stage 3, to further improve the metamodel accuracy, local refinement around MPP is accomplished as shown in Fig. 5 d). Obviously, the final CAL-ARBF metamodel displays an accurate approximation to LSF and the generated samples shows excellent space distribution performance.

Based on the established CAL-ARBF metamodel and MCS, the failure probability is calculated. The convergence stages of failure probability and MCS samples distribution are depicted in Fig. 6. From Fig. 6, we find that the CAL-ARBF metamodel can acquire an accurate result with only 12 samples, which shows the proposed approach holds the ability of acquiring accurate result efficiently. Moreover, to further validate the computing advantages of CAL-ARBF metamodel, Table 2 compares the results from the direct MCS, CAL-ARBF metamodel in different stages. It shows



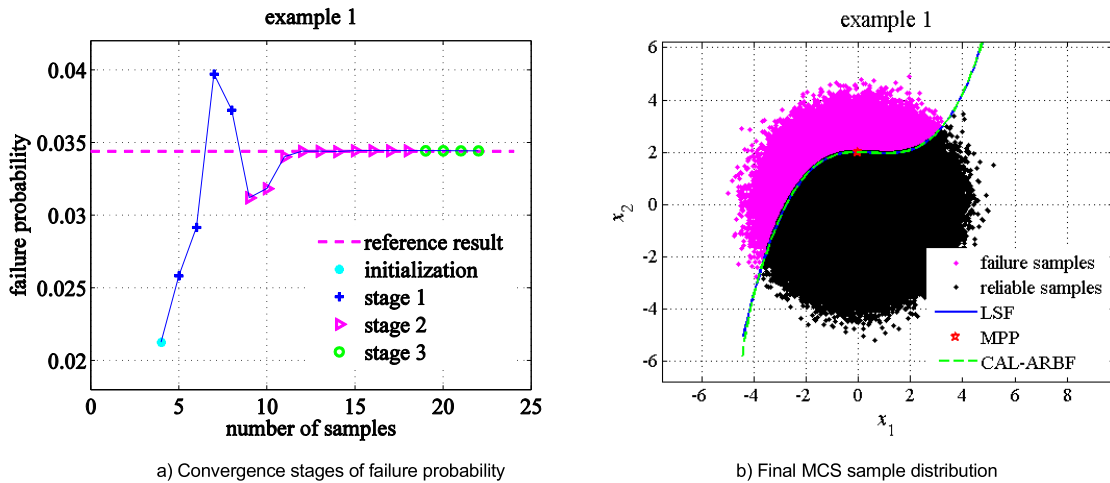


FIGURE 6. Failure probability evaluation (example 1,  $\lambda^* = 0.7$ ).

TABLE 2. Result comparisons of failure probabilities (example 1,  $\lambda^* = 0.7$ ).

Method	$p_f (10^{-2})$	$N_s$	$C_V (10^{-2})$	$\delta_1 (10^{-4})$
Direct MCS	3.443	$5 \times 10^6$	0.237	—
CAL-ARBF (stage 1)	3.724	8	0.237	816.149
CAL-ARBF (stage 2)	3.444	18	0.237	2.904
CAL-ARBF (stage 3)	3.443	22	0.237	0

that CAL-ARBF metamodel can improve the approximation accuracy gradually and CAL-ARBF metamodel in stage 3 holds the highest approximation accuracy.

**B. EXAMPLE 2: A LOCAL NONLINEAR PROBLEM**

To demonstrate the local approximation ability of the CAL-ARBF metamodel, a local nonlinear problem is employed [38]:

$$g(x) = x_1^3 + x_2^3 - 18 \tag{18}$$

where input variables  $x_1$  and  $x_2$  both follow normal distribution, whose mean values are 10 and 9.9 respectively and the standard deviations of them are both set as 5. With different adjustment coefficients ( $\lambda^* = 0.6, 0.7, 0.8, 0.9$ ), the reliability analysis of this example is performed by CAL-ARBF metamodel. The samples distributions and reliability analysis results are acquired in Fig. 7 and Table 3 respectively. Herein, the blue dotted line arcs in Fig. 7 represent the region containing the MCS samples and the radius is calculated by  $\max \|x_{MCSi}\|_2$ .

Fig. 7 shows that a large adjustment coefficient can constrain new samples being generated around the NCP or MPP, which can avoid the samples being out of the sensitive region and thereby improves the efficiency, whereas a small value can keep the samples being distant with each other and distributed uniformly along LSF, so it can improve the fitting precision overall the sensitive region. Furthermore, we also

TABLE 3. Results of failure probabilities with different adjustment coefficients (example 2).

Method	$p_f (10^{-3})$	$N_s$	$C_V (10^{-2})$	$\delta_1 (10^{-4})$
Direct MCS	5.713	$5 \times 10^6$	0.590	—
CAL-ARBF ( $\lambda^*=0.6$ )	5.713	27	0.590	0
CAL-ARBF ( $\lambda^*=0.7$ )	5.713	28	0.590	0
CAL-ARBF ( $\lambda^*=0.8$ )	5.714	31	0.590	1.750
CAL-ARBF ( $\lambda^*=0.9$ )	5.709	26	0.590	7.002

discover that CAL-ARBF metamodel with all adjustment coefficients ( $\lambda^* = 0.6, 0.7, 0.8, 0.9$ ) achieve excellent samples distributions and precise approximations. Table 3 shows that the results obtained with CAL-ARBF metamodel under different adjustment coefficients can all hold high accuracy, which demonstrates the robustness of the proposed method.

To illustrate the metamodeling procedure, the CAL-ARBF metamodeling stages with  $\lambda^* = 0.7$  is shown in Fig. 8 (4 extra samples used to generate the NCP): Along with the increasing of new samples overall the sensitive region iteratively, the CAL-ARBF metamodel can accurately approximate the LSF with local nonlinear characteristics gradually. The final metamodel curve show that the proposed CAL-ARBF possesses a high fitting precision for local nonlinear problems. According to the constructed CAL-ARBF metamodel, the failure probability evaluation is performed. The analysis results are depicted in Fig. 9. It illustrates that the CAL-ARBF metamodel can achieve an accurate failure probability with only 20 samples, which shows its ability of performing reliability analysis efficiently. Moreover, to validate the superiority of CAL-ARBF metamodel, Table 4 compares the analysis results from direct MCS, CAL-ARBF in different stages, active refinement-based adaptive Kriging surrogate model (AR-AKSM) [38]. It demonstrates that the CAL-ARBF metamodel in stage 3 holds the highest approximation accuracy and local refinement in stage 3 can improve the accuracy greatly.

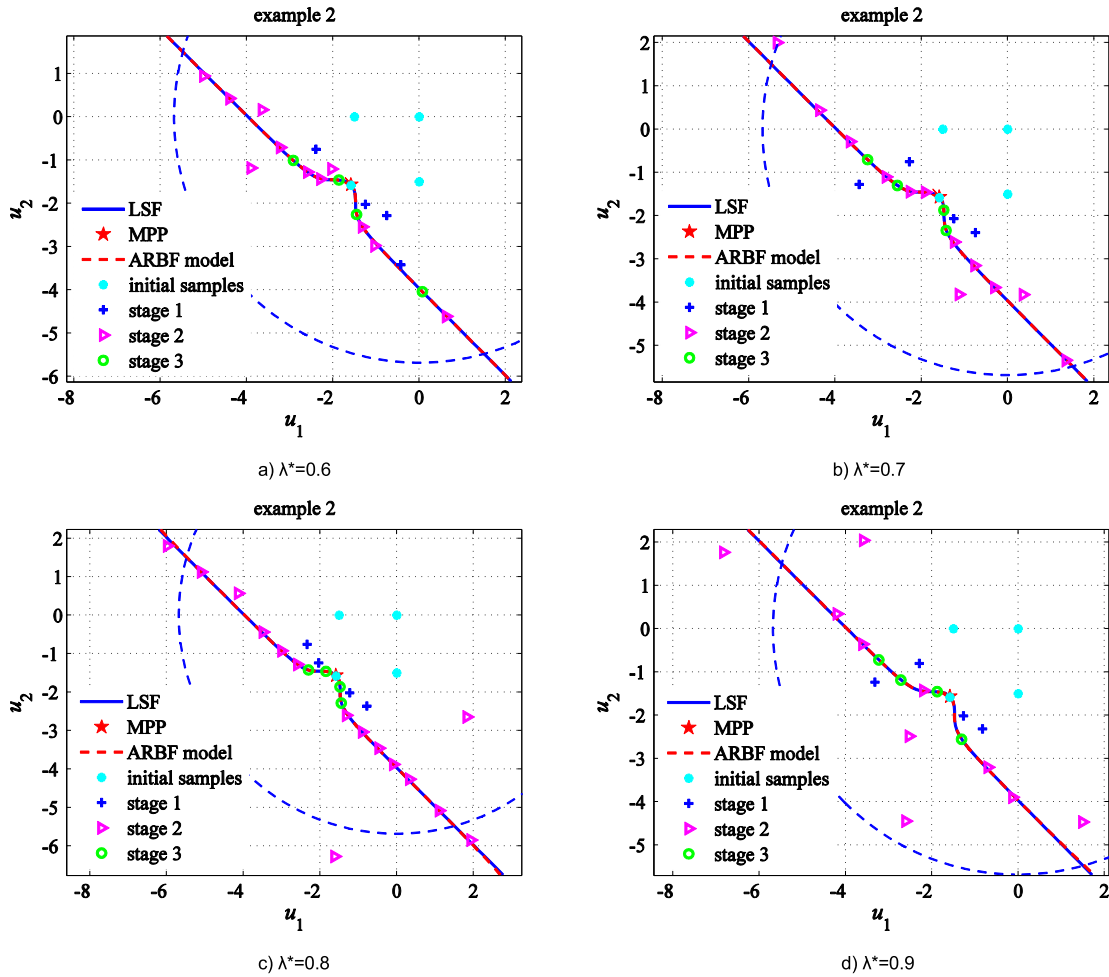


FIGURE 7. Sample distribution with different adjustment coefficients (example 2).

TABLE 4. Result comparisons of failure probabilities (example 2,  $\lambda^* = 0.7$ ).

Method	$p_f (10^{-3})$	$N_s$	$C_v (10^{-2})$	$\delta_1 (10^{-4})$
Direct MCS	5.713	$5 \times 10^6$	0.590	—
CAL-ARBF (stage 1)	8.290	9	0.489	4511.115
CAL-ARBF (stage 2)	5.709	24	0.590	7.732
CAL-ARBF (stage 3)	5.713	28	0.590	0
AR-AKSM	5.711	45	2.1	3.501

C. EXAMPLE 3: A NONLINEAR OSCILLATOR

To verify the moderate dimensional processing ability of CAL-ARBF metamodel, a nonlinear oscillator with 6 input variables is introduced as shown in Fig. 10 [35], [39], [40]. The performance function is expressed as:

$$g(c_1, c_2, m, r, t_1, F_1) = 3r - \left| \frac{2F_1}{mw_0^2} \sin\left(\frac{w_0 t_1}{2}\right) \right| \quad (19)$$

where  $w_0$  is  $\sqrt{(c_1 + c_2)/m}$  and  $c_1, c_2, m, r, t_1, F_1$  are regarded as random input variables. The distribution characteristics of them are illustrated in Table 5.

Through the CAL-ARBF metamodels under different adjustment coefficients ( $\lambda^* = 0.6, 0.7, 0.8, 0.9$ ), the failure probability evaluation of nonlinear oscillator is accomplished (5 extra samples used to obtain NCP). The results are listed in Table 6. It can be seen that all the results hold high accuracy compared with direct MCS, which illustrates that the adjustment coefficient has little influence on the computational accuracy for structural reliability analysis. By choosing adjustment coefficient  $\lambda^* = 0.8$ , the convergence stages of failure probability are obtained in Fig. 11. It can be seen that the CAL-ARBF metamodel can acquire accurate results by about 40 samples, which shows that the proposed method holds the ability of performing reliability analysis efficiently.

To demonstrate the superiority of CAL-ARBF metamodeling, several state-of-the-art methods are compared in Table 7. It shows that the CAL-ARBF metamodel holds the highest computational accuracy. However, due to the convergence conditions in stage 2 (minimum sample number is  $5n$ ), the proposed method needs more samples than global sensitivity analysis-enhanced surrogate method (GSAS) [35] and cross-validation-based sequential sampling

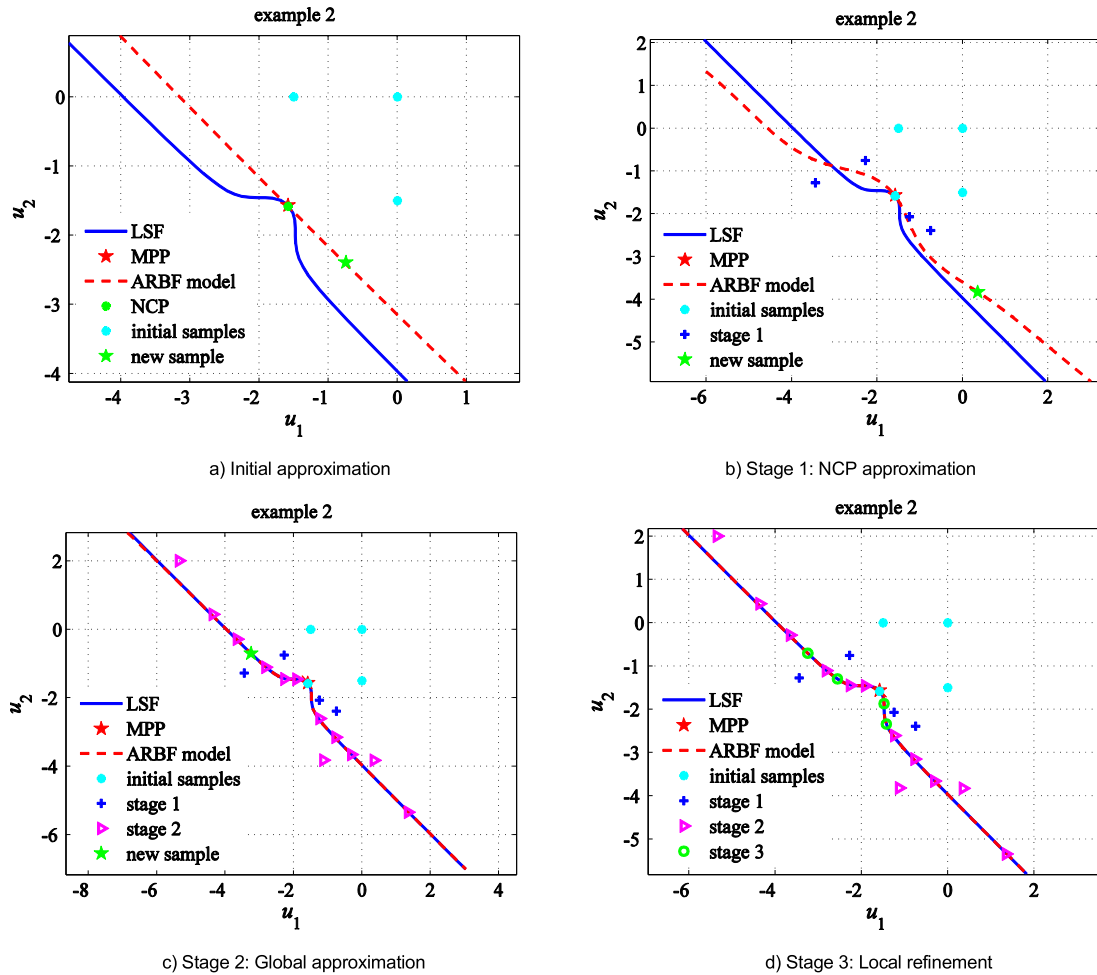


FIGURE 8. Metamodeling stages of CAL-ARBF (example 2,  $\lambda^* = 0.7$ ).

TABLE 5. Distribution characteristics of random variables.

Random variables	Distribution type	Mean	Standard deviation
$M$	Normal	1	0.05
$c_1$	Normal	1	0.1
$c_2$	Normal	0.1	0.01
$R$	Normal	0.5	0.05
$t_1$	Normal	1	0.2
$F_1$	Normal	1	0.2

TABLE 6. Results of failure probabilities with different adjustment coefficients (example 3).

Method	$p_f (10^{-2})$	$N_s$	$C_V (10^{-2})$	$\delta_1 (10^{-4})$
Direct MCS	2.860	$5 \times 10^6$	0.24	—
CAL-ARBF ( $\lambda^*=0.6$ )	2.859	67	0.24	3.500
CAL-ARBF ( $\lambda^*=0.7$ )	2.862	69	0.24	6.993
CAL-ARBF ( $\lambda^*=0.8$ )	2.861	67	0.24	3.500
CAL-ARBF ( $\lambda^*=0.9$ )	2.861	68	0.24	3.500

method (CV-SSM) [39]. Moreover, compared with distance-based learning function (DBLF) [40], variance-based learning function method (CBLF) [40] and mixed

TABLE 7. Result comparisons of failure probabilities (Example 3,  $\lambda^* = 0.8$ ).

Method	$p_f (10^{-2})$	$N_s$	$C_V (10^{-2})$	$\delta_1 (10^{-3})$
Direct MCS	2.860	$5 \times 10^6$	0.26	—
CAL-ARBF (stage 2)	2.864	55	0.26	1.399
CAL-ARBF (stage 3)	2.861	67	0.26	0.350
GSAS	2.86	44	—	—
CV-SSM $a=0.3$	2.877	55.90	0.82	5.944
CV-SSM $a=0.5$	2.867	59.60	0.82	2.448
DBLF	2.841	92.30	0.83	6.643
$\psi_d$	2.855	93.10	0.82	1.748
VBLF	2.855	93.10	0.82	1.748
MLF ( $a=0.5$ )	2.868	94.2	0.82	2.797

Note that  $a$  is the related coefficients in the learning functions.

learning function method (MLF) [40], the CAL-ARBF metamodel holds the computational advantages in both efficiency and accuracy. To sum up, the comparisons results demonstrate that the CAL-ARBF metamodel can address the moderate dimensional problems with high accuracy and efficiency.

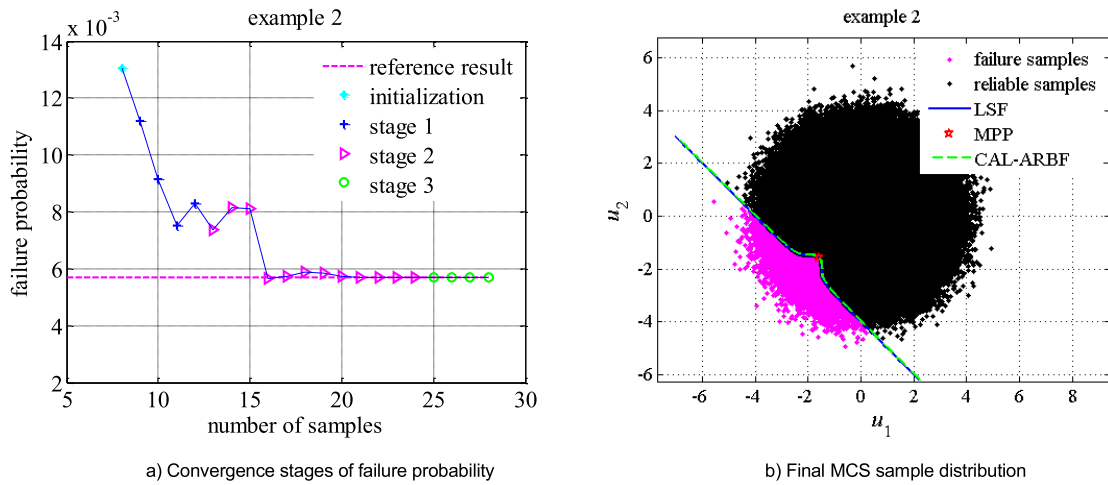


FIGURE 9. Failure probability evaluation (example 2,  $\lambda^* = 0.7$ ).

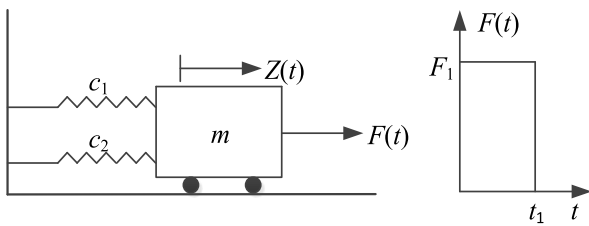


FIGURE 10. A nonlinear oscillator.

D. EXAMPLE 4: A TRUSS STRUCTURE

To verify the ability of CAL-ARBF metamodel in dealing with high-dimensional problems, a practical engineering structure with 18 input variables as shown in Fig. 12 is used, whose performance function is implicit. 15 cross-sectional areas and 3 external loads are considered as input random variables, whose distribution characteristics are illustrated in Table 8. Moreover, the elastic modulus is regarded as a deterministic parameter, whose value is set as 200 GPa. The random response at risk point is  $D(x)$  and the allowance displacement is 7.5 cm. Then the performance function  $g(x)$  of the truss structure is expressed as:

$$g(x) = 7.5 - D(x) \tag{20}$$

The failure probability evaluation of the truss structure is executed with CAL-ARBF metamodel under different adjustment coefficients ( $\lambda^* = 0.6, 0.7, 0.8, 0.9$ ) and 4 extra samples are used to obtain the NCP. The results are listed in Table 9. It shows that the CAL-ARBF metamodel can obtain highly accurate results with all of adjustment coefficients. Moreover, since the failure probabilities listed in table 9 are accurate enough for practical engineering, the most efficient method ( $\lambda^* = 0.8$ ) is utilized to analysis the proposed method in detail, and the failure probability is obtained as  $1.375 \times 10^{-3}$  after 192 performance function executions. The convergence stages of failure probability are drawn in Fig. 13, which

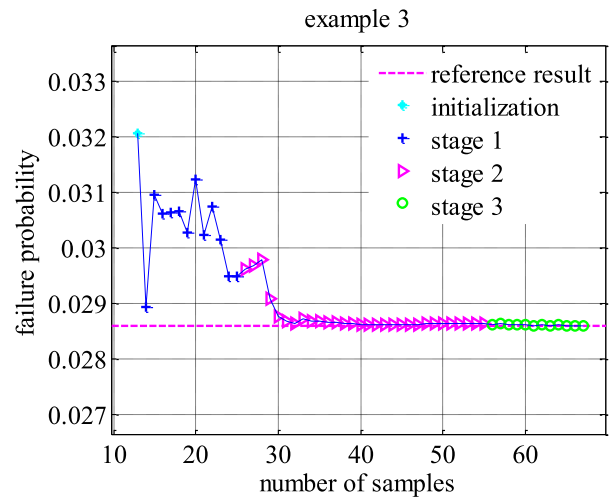


FIGURE 11. Convergence stages of failure probability (example 3,  $\lambda^* = 0.8$ ).

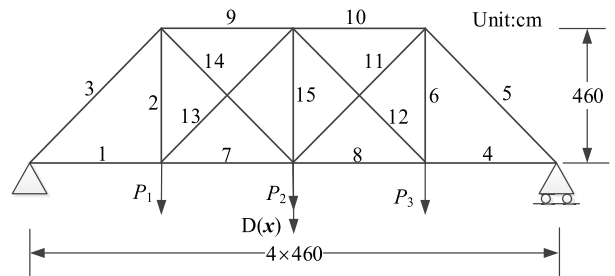


FIGURE 12. A 15-member truss structure.

shows that the CAL-ARBF can achieve accurate results iteratively.

To validate the advantages of the proposed CAL-ARBF metamodel, we compare the analysis results of CAL-ARBF metamodel with that of adaptive importance sampling method (AIS) [59], shifted importance sampling method

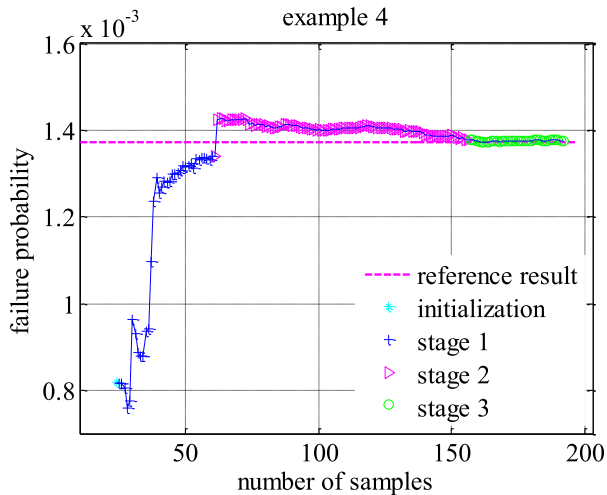


FIGURE 13. Convergence stages of failure probability (example 4,  $\lambda^* = 0.8$ ).

TABLE 8. Distribution characteristics of random variables.

Random variables	Distribution type	Mean	Standard deviation
$A_1$ - $A_6$ (cm <sup>2</sup> )	Normal	10.32	0.516
$A_7$ - $A_{15}$ (cm <sup>2</sup> )	Normal	6.45	0.323
$P_1$ (kN)	Log-normal	88.94	8.894
$P_2$ (kN)	Log-normal	266.92	26.692
$P_3$ (kN)	Log-normal	88.94	8.894

TABLE 9. Results of failure probabilities with different adjustment coefficients (example 4).

Method	$p_f (10^{-3})$	$N_s$	$C_V (10^{-2})$	$\delta_1 (10^{-4})$
Direct MCS	1.372	$5 \times 10^6$	1.207	—
CAL-ARBF ( $\lambda^*=0.6$ )	1.380	208	1.207	58.31
CAL-ARBF ( $\lambda^*=0.7$ )	1.375	193	1.205	21.87
CAL-ARBF ( $\lambda^*=0.8$ )	1.375	192	1.206	21.87
CAL-ARBF ( $\lambda^*=0.9$ )	1.373	245	1.205	7.29

TABLE 10. Result comparisons of failure probabilities (example 4,  $\lambda^* = 0.8$ ).

Method	$p_f (10^{-3})$	$N_s$	$C_V (10^{-2})$	$\delta_1 (10^{-3})$
Direct MCS	1.372	$5 \times 10^6$	1.207	—
CAL-ARBF (stage 2)	1.379	157	1.203	5.10
CAL-ARBF (stage 3)	1.375	192	1.206	2.19
AIS	1.34	117349	—	23.32
SIS	1.37	47111	—	1.46
CIS-RSM	1.20	2102	—	125.36

(SIS) [59] and the combination of importance sampling and RSM (CIS-RSM) [59]. The comparison results are summarized in Table 10. Obviously, the CAL-ARBF holds the highest computational accuracy than AIS, SIS and CIS-RSM, and nearly be consistent with direct MCS. For computational efficiency, the CAL-ARBF, AIS, SIS and CIS-RSM possess higher simulation efficiency than direct MCS, yet the required samples of CAL-ARBF is far

less than AIS, SIS and CIS-RSM. Therefore, it is validated that the developed CAL-ARBF approach can accurately and efficiently address the implicit reliability analysis problem.

#### IV. CONCLUSION

In this paper, a new reliability analysis approach (CAL-ARBF) based on collaborative active learning strategy (CAL) and augmented radial basis function metamodel (ARBF) is presented. Through describing the region constraint, surface constraint and distance constraint mathematically and collaborating them in a collaborative active learning framework, the CAL function is formulated to generate new samples with excellent space distribution. Combined with ARBF metamodel, the CAL-ARBF metamodel is completed iteratively. Through method comparisons in four typical examples, the efficiency and accuracy advantages of CAL-ARBF metamodel approach are validated. Some conclusions are derived as follows:

(1) The generated samples distribution reveals that the presented CAL strategy can constrain new samples be generated in sensitivity region, near limit state surface and keep certain distances mutually.

(2) From convergence stages comparisons, we discover that the local refinement stage in CAL strategy can effectively improve approximation accuracy, especially for local nonlinear problems.

(3) From method comparisons in four examples, we find that the proposed CAL-ARBF metamodel hold higher efficiency and accuracy for reliability analysis compared with several state-of-the-art approaches.

The proposed method CAL-ARBF provides an accurate and efficient approach to perform reliability analysis for the practical engineering structures. Though the MPP is inaccurate during the iterative process, the CAL-ARBF can still perform reliability analysis accurately and efficiently. In the future, considering the MPP is evaluated during iterative process, the CAL-ARBF can be combined with the importance sampling to deal with the problems with low failure probabilities, and it can also cooperate with multiple MPPs evaluating technique to deal with the problems with multiple MPPs.

#### REFERENCES

- [1] S. P. Zhu, Q. Liu, Q. Lei, and Q. Wang, "Probabilistic fatigue life prediction and reliability assessment of a high pressure turbine disc considering load variations," *Int. J. Damage Mech.*, vol. 27, no. 10, pp. 1569–1588, Nov. 2018.
- [2] B. Keshtegar, "A hybrid conjugate finite-step length method for robust and efficient reliability analysis," *Appl. Math. Model.*, vol. 45, pp. 226–237, May 2017.
- [3] L.-K. Song, J. Wen, C.-W. Fei, and G.-C. Bai, "Distributed collaborative probabilistic design of multi-failure structure with fluid-structure interaction using fuzzy neural network of regression," *Mech. Syst. Signal Process.*, vol. 104, pp. 72–86, May 2018.
- [4] C. Lu, Y.-W. Feng, C.-W. Fei, and S. Bu, "Decomposed-coordinated framework with enhanced extremum Kriging for multicomponent dynamic probabilistic failure analyses," *IEEE Access*, vol. 7, pp. 163287–163300, 2019.



- [5] S. P. Zhu, Q. Liu, J. Zhou, and Z. Y. Yu, "Fatigue reliability assessment of turbine discs under multi-source uncertainties," *Fatigue Fract. Eng. Mater. Struct.*, vol. 41, no. 6, pp. 1291–1305, Jan. 2018.
- [6] Y. Wei, G. Bai, L. Song, and B. Bai, "The estimation of reliability probability of structures based on improved iterative response surface methods," *KSCCE J. Civil Eng.*, vol. 23, no. 9, pp. 4063–4074, Sep. 2019.
- [7] C. Jiang, H. Qiu, Z. Yang, L. Chen, L. Gao, and P. Li, "A general failure-pursuing sampling framework for surrogate-based reliability analysis," *Rel. Eng. Syst. Saf.*, vol. 183, pp. 47–59, Mar. 2019.
- [8] L.-K. Song, G.-C. Bai, and C.-W. Fei, "Probabilistic LCF life assessment for turbine discs with DC strategy-based wavelet neural network regression," *Int. J. Fatigue*, vol. 119, pp. 204–219, Feb. 2019.
- [9] Y. Duan, W. Li, X. Fu, Y. Luo, and L. Yang, "A methodology for reliability of WSN based on software defined network in adaptive industrial environment," *IEEE/CAA J. Automatica Sinica*, vol. 5, no. 1, pp. 74–82, Jan. 2018.
- [10] Z. Ding, Y. Zhou, G. Pu, and M. Zhou, "Online failure prediction for railway transportation systems based on fuzzy rules and data analysis," *IEEE Trans. Rel.*, vol. 67, no. 3, pp. 1143–1158, Sep. 2018.
- [11] P. Bjerager, "Probability integration by directional simulation," *J. Eng. Mech.*, vol. 114, no. 8, pp. 1285–1302, 1988.
- [12] C. G. Bucher and U. Bourgund, "A fast and efficient response surface approach for structural reliability problems," *Struct. Saf.*, vol. 7, no. 1, pp. 57–66, Jan. 1990.
- [13] W. T. Zhao and Z. P. Qiu, "An efficient response surface method and its application to structural reliability and reliability-based optimization," *Finite Elements Anal. Des.*, vol. 67, pp. 34–42, May 2013.
- [14] D. L. Allaire and V. I. Carbone, "An improvement of the response surface method," *Struct. Saf.*, vol. 33, no. 2, pp. 165–172, 2011.
- [15] L.-K. Song, C.-W. Fei, J. Wen, and G.-C. Bai, "Multi-objective reliability-based design optimization approach of complex structure with multi-failure modes," *Aerosp. Sci. Technol.*, vol. 64, pp. 52–62, May 2017.
- [16] J. Cheng, Q. S. Li, and R.-C. Xiao, "A new artificial neural network-based response surface method for structural reliability analysis," *Probabilistic Eng. Mech.*, vol. 23, no. 1, pp. 51–63, Jan. 2008.
- [17] L.-K. Song, C.-W. Fei, G.-C. Bai, and L.-C. Yu, "Dynamic neural network method-based improved PSO and BR algorithms for transient probabilistic analysis of flexible mechanism," *Adv. Eng. Informat.*, vol. 33, pp. 144–153, Aug. 2017.
- [18] X.-H. Tan, W.-H. Bi, X.-L. Hou, and W. Wang, "Reliability analysis using radial basis function networks and support vector machines," *Comput. Geotechn.*, vol. 38, no. 2, pp. 178–186, Mar. 2011.
- [19] U. Alibrandi, A. M. Alani, and G. Ricciardi, "A new sampling strategy for SVM-based response surface for structural reliability analysis," *Probabilistic Eng. Mech.*, vol. 41, pp. 1–12, Jul. 2015.
- [20] C. Lu, Y.-W. Feng, R. P. Liem, and C.-W. Fei, "Improved Kriging with external response surface method for structural dynamic reliability and sensitivity analyses," *Aerosp. Sci. Technol.*, vol. 76, pp. 164–175, May 2018.
- [21] L.-K. Song, G.-C. Bai, and C.-W. Fei, "Dynamic surrogate modeling approach for probabilistic creep-fatigue life evaluation of turbine disks," *Aerosp. Sci. Technol.*, vol. 95, Dec. 2019, Art. no. 105439.
- [22] X. Li, C. Gong, L. Gu, W. Gao, Z. Jing, and H. Su, "A sequential surrogate method for reliability analysis based on radial basis function," *Struct. Saf.*, vol. 73, pp. 42–53, Jul. 2018.
- [23] Q. Wang and H. Fang, "Reliability analysis of tunnels using an adaptive RBF and a first-order reliability method," *Comput. Geotechn.*, vol. 98, pp. 144–152, Jun. 2018.
- [24] A. Hadidi, B. F. Azar, and A. Rafiee, "Efficient response surface method for high-dimensional structural reliability analysis," *Struct. Saf.*, vol. 68, pp. 15–27, Sep. 2017.
- [25] L. Shi, B. Sun, and D. S. Ibrahim, "An active learning reliability method with multiple kernel functions based on radial basis function," *Struct. Multidisciplinary Optim.*, vol. 60, no. 1, pp. 211–229, Jul. 2019.
- [26] L. K. Song, G. C. Bai, and C. W. Fei, "Multi-failure probabilistic design for turbine bladed disks using neural network regression with distributed collaborative strategy," *Aerosp. Sci. Technol.*, vol. 92, pp. 464–477, Sep. 2019.
- [27] M. Q. Chau, X. Han, C. Jiang, Y. C. Bai, T. N. Tran, and V. H. Truong, "An efficient PMA-based reliability analysis technique using radial basis function," *Eng. Computations*, vol. 31, no. 6, pp. 1098–1115, Jul. 2014.
- [28] H. Fang and M. F. Horstemeyer, "Global response approximation with radial basis functions," *Eng. Optim.*, vol. 38, no. 4, pp. 407–424, Jun. 2006.
- [29] J. Eason and S. Cremaschi, "Adaptive sequential sampling for surrogate model generation with artificial neural networks," *Comput. Chem. Eng.*, vol. 68, pp. 220–232, Sep. 2014.
- [30] V. Dubourg, B. Sudret, and F. Deheeger, "Metamodel-based importance sampling for structural reliability analysis," *Probabilistic Eng. Mech.*, vol. 33, pp. 47–57, Jul. 2013.
- [31] B. J. Bichon, M. S. Eldred, L. P. Swiler, S. Mahadevan, and J. M. McFarland, "Efficient global reliability analysis for nonlinear implicit performance functions," *AIAA J.*, vol. 46, no. 10, pp. 2459–2468, Oct. 2008.
- [32] V. Picheny, D. Ginsbourger, O. Roustant, R. T. Haftka, and N.-H. Kim, "Adaptive designs of experiments for accurate approximation of a target region," *J. Mech. Des.*, vol. 132, no. 7, Jul. 2010, Art. no. 071008.
- [33] B. Echard, N. Gayton, and M. Lemaire, "AK-MCS: An active learning reliability method combining Kriging and Monte Carlo simulation," *Struct. Saf.*, vol. 33, no. 2, pp. 145–154, Mar. 2011.
- [34] Z. Wen, H. Pei, H. Liu, and Z. Yue, "A sequential Kriging reliability analysis method with characteristics of adaptive sampling regions and parallelizability," *Rel. Eng. Syst. Saf.*, vol. 153, pp. 170–179, Sep. 2016.
- [35] Z. Hu and S. Mahadevan, "Global sensitivity analysis-enhanced surrogate (GSAS) modeling for reliability analysis," *Structural Multidisciplinary Optim.*, vol. 53, no. 3, pp. 501–521, Mar. 2016.
- [36] Z. Peijuan, W. C. Ming, Z. Zhouhong, and W. Liqi, "A new active learning method based on the learning function u of the AK-MCS reliability analysis method," *Eng. Struct.*, vol. 148, pp. 185–194, Oct. 2017.
- [37] Z. Sun, J. Wang, R. Li, and C. Tong, "LIF: A new Kriging based learning function and its application to structural reliability analysis," *Rel. Eng. Syst. Saf.*, vol. 157, pp. 152–165, Jan. 2017.
- [38] B. Gaspar, A. P. Teixeira, and C. G. Soares, "Adaptive surrogate model with active refinement combining Kriging and a trust region method," *Rel. Eng. Syst. Saf.*, vol. 165, pp. 277–291, Sep. 2017.
- [39] N.-C. Xiao, M. J. Zuo, and W. Guo, "Efficient reliability analysis based on adaptive sequential sampling design and cross-validation," *Appl. Math. Model.*, vol. 58, pp. 404–420, Jun. 2018.
- [40] N.-C. Xiao, M. J. Zuo, and C. Zhou, "A new adaptive sequential sampling method to construct surrogate models for efficient reliability analysis," *Rel. Eng. Syst. Saf.*, vol. 169, pp. 330–338, Jan. 2018.
- [41] X. Yang, Y. Liu, X. Fang, and C. Mi, "Estimation of low failure probability based on active learning Kriging model with a concentric ring approaching strategy," *Struct. Multidisciplinary Optim.*, vol. 58, no. 3, pp. 1175–1186, Sep. 2018.
- [42] W. Yun, Z. Lu, K. Feng, and X. Jiang, "A novel step-wise AK-MCS method for efficient estimation of fuzzy failure probability under probability inputs and fuzzy state assumption," *Eng. Struct.*, vol. 183, pp. 340–350, Mar. 2019.
- [43] J. Zhang, M. Xiao, L. Gao, and J. Fu, "A novel projection outline based active learning method and its combination with Kriging metamodel for hybrid reliability analysis with random and interval variables," *Comput. Methods Appl. Mech. Eng.*, vol. 341, pp. 32–52, Nov. 2018.
- [44] L. Martino, J. Vicent, and G. Camps-Valls, "Automatic emulator and optimized look-up table generation for radiative transfer models," in *Proc. IEEE Int. Geosci. Remote Sens. Symp.*, Jul. 2017, pp. 1457–1460.
- [45] D. Busby, "Hierarchical adaptive experimental design for Gaussian process emulators," *Rel. Eng. Syst. Saf.*, vol. 94, no. 7, pp. 1183–1193, Jul. 2009.
- [46] J. Verrelst, S. Dethier, J. P. Rivera, J. Muñoz-Marí, G. Camps-Valls, and J. Moreno, "Active learning methods for efficient hybrid biophysical variable retrieval," *IEEE Geosci. Remote Sens. Lett.*, vol. 13, no. 7, pp. 1012–1016, Jul. 2016.
- [47] D. H. Svendsen, L. Martino, and G. Camps-Valls, "Active emulation of computer codes with Gaussian processes—Application to remote sensing," *Pattern Recognit.*, vol. 100, pp. 1–12, Apr. 2020.
- [48] G. D. S. Ferreira and D. Gamerman, "Optimal design in geostatistics under preferential sampling," *Bayesian Anal.*, vol. 10, no. 3, pp. 711–735, Sep. 2015.
- [49] J. Zhang, M. Xiao, L. Gao, and S. Chu, "A combined projection-outline-based active learning Kriging and adaptive importance sampling method for hybrid reliability analysis with small failure probabilities," *Comput. Methods Appl. Mech. Eng.*, vol. 344, pp. 13–33, Feb. 2019.
- [50] J. Zhang, M. Xiao, and L. Gao, "An active learning reliability method combining Kriging constructed with exploration and exploitation of failure region and subset simulation," *Rel. Eng. Syst. Saf.*, vol. 188, pp. 90–102, Aug. 2019.

- [51] M. Xiao, J. Zhang, L. Gao, S. Lee, and A. T. Eshghi, "An efficient Kriging-based subset simulation method for hybrid reliability analysis under random and interval variables with small failure probability," *Struct. Multidisciplinary Optim.*, vol. 59, no. 6, pp. 2077–2092, Jun. 2019.
- [52] F. Vandenbergh and A. Engelbrecht, "A study of particle swarm optimization particle trajectories," *Inf. Sci.*, vol. 176, no. 8, pp. 937–971, Apr. 2006.
- [53] W. C. Zhong, J. Liu, M. Z. Xue, and L. Jiao, "A multiagent genetic algorithm for global numerical optimization," *IEEE Trans. Syst., Man, Cybern. B, Cybern.*, vol. 34, no. 2, pp. 1128–1141, Apr. 2004.
- [54] D. Karaboga and B. Akay, "A comparative study of artificial bee colony algorithm," *Appl. Math. Comput.*, vol. 214, no. 1, pp. 108–132, Aug. 2009.
- [55] Y. Feng, M. Zhou, G. Tian, Z. Li, Z. Zhang, Q. Zhang, and J. Tan, "Target disassembly sequencing and scheme evaluation for CNC machine tools using improved multiobjective ant colony algorithm and fuzzy integral," *IEEE Trans. Syst., Man, Cybern. Syst.*, vol. 49, no. 12, pp. 2438–2451, Dec. 2019.
- [56] J. Wang and T. Kumbasar, "Parameter optimization of interval type-2 fuzzy neural networks based on PSO and BBBC methods," *IEEE/CAA J. Automatica Sinica*, vol. 6, no. 1, pp. 247–257, Jan. 2019.
- [57] S. C. Gao, M. C. Meng, Y. R. Wang, J. J. Cheng, H. Yachi, and J. H. Wang, "Dendritic neuron model with effective learning algorithms for classification, approximation and prediction," *IEEE Trans. Neural Netw. Learn. Syst.*, vol. 30, no. 2, pp. 601–614, Feb. 2019.
- [58] P. Y. Zhang, S. Shu, and M. C. Zhou, "An online fault detection method based on SVM-grid for cloud computing systems," *IEEE/CAA J. Automatica Sinica*, vol. 5, no. 2, pp. 445–456, Mar. 2018.
- [59] M. A. Shayanfar, M. A. Barkhordari, and M. A. Roudak, "An efficient reliability algorithm for locating design point using the combination of importance sampling concepts and response surface method," *Commun. Nonlinear Sci. Numer. Simul.*, vol. 47, pp. 223–237, Jun. 2017.



**YANXU WEI** was born in Hebei, China, in 1987. He received the B.S. degree in mechanical engineering and automation and the M.S. degree in mechanical design and theory from the Taiyuan University of Science and Technology, China, in 2012 and 2015, respectively. He is currently pursuing the Ph.D. degree with the School of Beihang University. His research interests include reliability evaluation, sensitivity analysis, design optimization, and mechanical design.



**GUANGCHEN BAI** was born in Harbin, China, in 1962. He received the B.S. degree in mechanical design and theory from the Harbin University of Science and Technology, China, in 1983, and the Ph.D. degree in structural reliability assessment from the Harbin Institute of Technology, China, in 1993.

From 1993 to 1995, he was an Assistant Professor with the School of Astronautics, Harbin Institute of Technology. From 1995 to 2000, he was an Associate Professor with the School of Energy and Power Engineering, Beihang University, where he was a Professor with the School of Energy and Power Engineering, from 2000 to 2016. Since 2016, he has been a tenured Professor with the School of Energy and Power Engineering, Beihang University. He is the author of more than 100 articles. His research interests include fatigue reliability assessment, vibration reliability evaluation, and multidisciplinary design optimization. He was a member of the American Institute of Aeronautics and Astronautics (AIAA) and the Chinese Society of Aeronautics and Astronautics (CSAA). He is a reviewer of more than 20 journals, such as *Chinese Journal of Aeronautics*, *Reliability Engineering and System Safety*, and *Chinese Journal of Mechanical Engineering*.



**LU-KAI SONG** was born in Heze, China, in 1990. He received the B.S. degree in mechanical engineering and automation from Shandong Jiaotong University, in 2013, the M.S. degree in mechanical design and theory from the Harbin University of Science and Technology, in 2015, and the Ph.D. degree in aerospace engineering from Beihang University, in 2020.

He is currently a Postdoctoral Fellow with the Research Institute of Aero-Engine, Beihang University. He is the author of more than 20 articles, including *Advanced Engineering Informatics*, *Mechanical Systems and Signal Processing*, and *International Journal of Fatigue*. He also holds six national patents. His research interests include surrogate modeling, reliability assessment, probabilistic fatigue design, and multidisciplinary design optimization with machine/deep learning for aircraft engines. He is a reviewer of more than ten journals, such as *IEEE Access*, *Aerospace Science and Technology*, and *Reliability Engineering and System Safety*.

...